OPTIMAL FIXTURING OF RIGID AND DEFORMABLE BODIES

W. Zhang, B. Salunkhe, P. G. Charalambides and U. Tasch
Department of Mechanical Engineering
University of Maryland, Baltimore County
Baltimore, MD 21228-5398

Abstract

As the first part of this work, a model initially developed for optimal grasping is being adopted to address optimal fixturing of a rigid workpiece. The model is tested using 2-D workpiece configurations used in other pilot studies reported in the literature. While verifying some of the findings reported elsewhere in the literature, the model also yielded other useful insights regarding optimal fixturing designs.

In an effort to establish the association between minimizing the normal maximum reaction force to minimizing the workpiece deformations, an energy criterion is employed to assess optimal fixturing conditions for a deformable workpiece subjected to drilling forces and moments. This second part of the study, is carried out with the aid of a simply supported beam which is fully constrained in the out-of-plane direction. The total elastic strain energy or work done by the drilling loads is calculated analytically as a function of the fixture clamping locations. Through a constrained energy minimization, optimal clamping locations have been obtained for a wide combination of a concentrated force, and a bi-axial bending moment. These loads simulate various manufacturing drilling processes. The reaction forces corresponding to the energy based optimal solutions were compared to reaction force solutions of non-optimal fixturing configurations.

The results suggest that, the energy based optimization does not necessarily yield minimal reaction forces at the clamping locations as suggested elsewhere. This energy-based optimization approach yields fixturing configurations which in addition to minimizing the energy of the deformable workpiece, in the decoupled loading cases also minimizes the deformations in the neighborhood of the drilling loads thus assuring higher accuracy of the manufacturing drilling process. With the aid of the simple beam workpiece, it is shown that, the method provides an attractive alternative for fixture optimization for one, two and possibly other analytically tractable three dimensional deformable workpieces.

1 Introduction

The quality and accuracy of manufacturing processes such as drilling or milling on a flexible or deformable workpiece depend on the fixturing which provides workpiece positioning and constraint. Fixtures are often designed by experienced engineers that utilize general guidelines and personal experience. Automated Fixturing Design (AFD) that is based on a CAD part model is a highly desired capability that industry is still lacking [1]. Initial fixturing design models were developed using rigid body kinematics addressing workpiece motion either under various geometrical constraints or aiming at inhibiting all workpiece motion [1-3]. In addition to the rigid body kinematics approach, recent studies [2-5] addressed fixture or grasping optimization through the minimization of an objective function mainly linked to the clamping reaction normal and tangential friction forces. The objective of those studies, was to select the clamping locations associated with statically admissible but optimized reaction forces exhibiting a minimum in the maximum normal reaction force. In those studies, it was hypothesized that minimizing the maximum normal reaction force led to fixturing designs which also minimized the workpiece deformations in the neighborhood of the manufacturing process and thus the energy of the workpiece. In other recent studies [6-8], the elasticity of the workpiece was incorporated into fixture optimizing algorithms. These methods mostly based on finite elements, used various fixture optimization criteria. Among others, these criteria included minimizing the elastic energy of the deformable workpiece or equivalently the work done on the deformable workpiece, minimizing a deformation index or a fixturing force or minimizing a maximum effective stress aiming at minimizing the damage induced by the manufacturing loads.

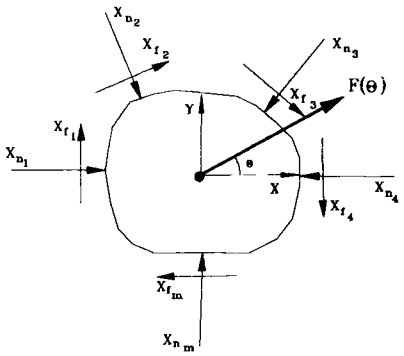

Fig. 1 A planar multifinger force closure, where x_n is the normal force and x_f the frictional one.

As discussed above, the freedom and constraint of rigid workpieces have been studied by the robotics community [9-10] that has addressed various grasping quality and stability issues. Although there are fundamental differences between the requirements of object grasping and workpiece fixturing [11], the mathematical formulation of the quality of a grasp [4-5] can be adopted to address the design of optimal fixturing. As the first part of this work, a model initially developed for optimal grasping is being adopted to address optimal fixturing of a rigid workpiece. The model is tested using 2-D workpiece configurations used in other pilot studies reported in the literature.

In an effort to establish the association between minimizing the normal maximum reaction force to minimizing the workpiece deformations, an energy criterion is employed to assess optimal fixturing conditions for a deformable workpiece subjected to drilling forces and moments. This second part of the study, is carried out with the aid of a simply supported beam which is fully constrained in the out-of-plane direction. As a result, and without loss of generality, the mechanical complexity reduces appreciably requiring knowledge of the mechanics of the deformable workpiece, i.e., the elastic beam, only within its plane. Furthermore, for slender beams, i.e., a height to length ratio $h/l \leq 10$, a mechanics of material approach can be employed in establishing the mechanics and thus solutions for the elastic energy stored in the deformable workpiece. Under the above conditions, the total elastic strain energy or work done by the drilling loads is calculated analytically as a function of the fixture clamping locations. Through a constrained energy minimization, optimal clamping locations can be obtained for a wide combination of a concentrated force, and a bi-axial bending moment. These loads are used to simulate various manufacturing drilling processes. The reaction forces corresponding to the energy based optimal solutions can then be compared to reaction force solutions of non-optimal fixturing configurations. Such a comparison will test the hypothesis used in rigid body fixturing models that minimizing the maximum normal reaction force leads to minimum deformations at the location of the manufacturing process. The grasping model adopted for optimal fixturing shall be presented next.

2 A grasping model adopted for optimal fixturing

For a planar multifinger force closure, shown in Figure 1, the grasping model can be expressed as:

$$G_n \cdot \underline{x}_n + G_f \cdot \underline{x}_f = \underline{F}(\theta) \tag{1}$$

where $\underline{x}_n \in \mathbb{R}^m$ and $\underline{x}_f \in \mathbb{R}^m$ are vectors of the normal and frictional finger forces, respectively, and $\underline{F}(\theta) \in \mathbb{R}^3$ is a vector of the generalized external load applied at the object along a given θ direction (in the planar case $0 \leq \theta \leq 2\pi$). G_n and $G_f \in \mathbb{R}^3 \times \mathbb{R}^m$ are the equilibrium balancing parameters that depend on the object geometry and contact characterization. In a physically realizable grip the normal finger forces ought to be non-negative

$$x_{n_i} \geq 0 \ , \ i = 1, ..., m \tag{2}$$

and if a Coulomb friction model is used $\underline{x}_n$ and $\underline{x}_f$ have to satisfy

$$|x_{f_i}| \leq \mu x_{n_i} \ , \ i = 1, ..., m \tag{3}$$

where μ is the static coefficient of friction.

Equations (1)-(3) constitute a force closure model, the solution of which does not necessarily exist. In fact in many practical applications, when a feasible solution does exist it may not be unique. Such ambiguity is often overcome by introducing a mathematical functional, that is minimized subject to constraints (1)-(3). Hershkovitz et al. [5] has selected convex functionals that address the ambiguity in the problem solution and furthermore generate grasping quality information. These functionals are:

$$H_1(\overline{x}_n) = \sum_{i=1}^{m} x_{n_i}^2 := ||\overline{x}_n||^2 \tag{4}$$

$$H_2(\overline{x}_n) := \max_{1 \leq i \leq m} |x_{n_i}| \tag{5}$$

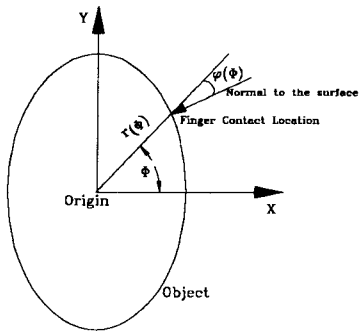

Fig. 2 The radial function $r(\phi)$ and surface normal direction $\varphi(\phi)$ capture the geometric description of a planar object that is single valued in polar coordinates.

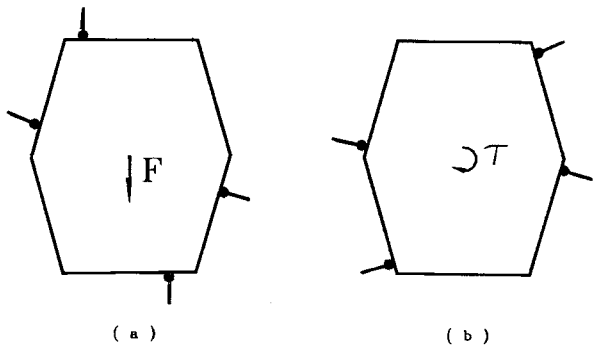

Fig. 3 Optimal fixture designs for a downward force F (a), and a clockwise torque τ (b). The values of the fixture indices are 0.718, and 0.048 [unit force], respectively.

$$H_3(\overline{x}_n) = \sum_{i=1}^{m}(x_{n_i}+1)\log(x_{n_i}+1) - \sum_{i=1}^{m} x_{n_i}. \quad (6)$$

$H_1(\overline{x}_n)$ is the square of the Euclidean-norm of the finger normal forces. It represents the energy level of linear systems, and in nonlinear domains $H_1(\overline{x}_n)$ has an energy-like characteristic. Human-beings tend to minimize their muscle efforts when performing force closures [12] and [13]. Such behavior is captured by minimizing $H_1(\overline{x}_n)$.

$H_2(\overline{x}_n)$ is an l_∞-norm of the normal finger forces. Obviously, large grasping forces may damage the object and it was demonstrated [12] and [13] that human-beings tend to avoid it. The minimization of $H_2(\overline{x}_n)$ simulates this grasping behavior. Notice that the selected $H_1(\overline{x}_n)$ and $H_2(\overline{x}_n)$ functionals are convex and therefore they possess global minima.

$H_3(\overline{x}_n)$ possesses the basic properties of an entropy function [14]. This function has a global minimum and for any non-negative $\overline{x}_n$, $H_3(\overline{x}_n) \geq 0$. In a recent study *Lee* and *Rim* [15] observed that, in force closures, the applied contact forces of the individual human fingers maintain fixed ratios. Hershkovitz [5] postulated that the different contributions of the fingers are due to their physiological variations. They further assumed that mechanical manipulators, that possess identical finger structures, generate high quality grasps when their contact forces are uniform. A uniform force distribution is obtained when $H_3(\overline{x}_n)$ is minimized.

Hence, three types of grasping quality measures that evaluate a grasp from three different perspectives have been proposed. These measures are based on the energy level of the gripper, the maximum finger force applied on the object, and the degree of uniformity of the grasping contact forces. The maximum applied finger force has also been the quantity that researchers, who address the development of fixture design algorithms, minimize [3]. In fact equations (1)-(3) together with objective function (5) is a generally accepted formulation for evaluating a fixturing index, that is analogous to the quality of a grasp.

When the geometrical description of the workpiece is incorporated into the force closure equations (1)-(3), one can recast the mathematical model as

$$G_n\left(\underline{\phi}, \underline{r}\left(\underline{\phi}\right), \varphi\left(\underline{\phi}\right)\right) \cdot \underline{x}_n\left(\underline{\phi}\right) + G_f\left(\underline{\phi}, \underline{r}\left(\underline{\phi}\right), \varphi\left(\underline{\phi}\right)\right) \cdot \underline{x}_f\left(\underline{\phi}\right) = \underline{F}(\theta) \quad (7)$$

$$x_{n_i}(\phi_i) \geq 0\ ,\ i = 1, \ldots, m \quad (8)$$

$$|x_{f_i}(\phi_i)| \leq \mu \cdot x_{n_i}(\phi_i)\ ,\ i = 1, \ldots, m \quad (9)$$

where m is the number of supports, $\underline{\phi} \in \mathbb{R}^m$ is a vector of the contact locations, and $\underline{x}_n\left(\underline{\phi}\right)$ and $\underline{x}_f\left(\underline{\phi}\right)$ $\in \mathbb{R}^m$ are vectors of the normal and frictional reaction forces. $\underline{r}\left(\underline{\phi}\right)$ and $\varphi\left(\underline{\phi}\right)$ are the radii and normal surface angles at the contact locations, and G_n and G_f $\in \mathbb{R}^3 \times \mathbb{R}^m$ are the equilibrium balancing parameters, that depend on the workpiece geometry and clamping locations. $\underline{F}(\theta)$ and μ follow the definitions of Equations (1) and (3). Here it is assumed that the object is planar and single valued in polar coordinates, as shown in Figure 2.

By minimizing an objective function (Equation 5) subject to the constraints expressed in Equations (7)-(9), one can identify m clamping locations that result

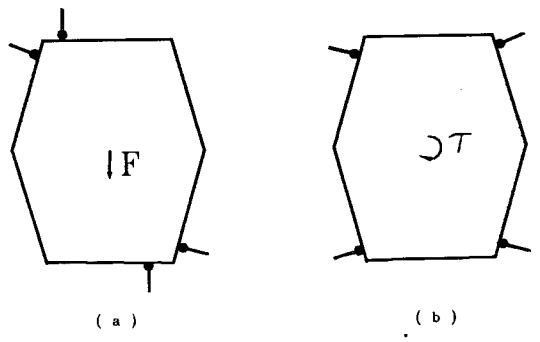

Fig. 4 Fixture designs for a downward force F (a), and a clockwise torque τ (b) that are suggested by Brost and Goldberg [3]. The values of the fixture indices are 0.825, and 0.056 [unit force], respectively.

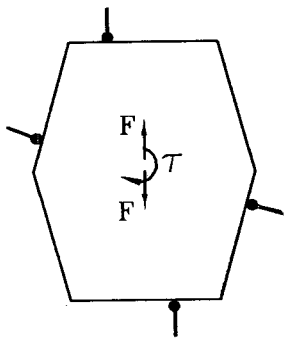

Fig. 5 Optimal fixture designs for a combination of upward and downward forces and a clockwise torque. This load combination represents a milling process, and the fixture index is 0.719 [unit force].

in the highest fixturing index value. This is done for a given manufacturing process and a known external load $\underline{F}(\theta)$. This formulation is used for selecting optimal fixture designs that support a prismatic workpiece, when (i) a downward force and (ii) a clockwise torque are applied. The optimal fixtures for the applied force and torque are shown in Figures 3(a) and 3(b), respectively. When the friction coefficient μ is set to 0.2, the corresponding values of the fixturing indices are 0.718 and 0.048 [unit force], respectively. Figure 4 depicts the fixtures selected by Brost and Goldberg [3] for the downward force (Figure 4(a)) and the clockwise torque (Figure 4(b)). The indices of these fixtures turn out to be 0.825 and 0.056 [unit force]. Hence, the fixture designs depicted in Figure 3 have better ratings than the fixtures selected in [3]. To further synthesize a milling process, a loading combination of up and downward forces and a clockwise torque is considered. The optimal fixture design for this case is shown in Figure 5 and its index value is 0.719 [unit force].

Hence, formulating the fixturing problem as a constraint optimization (Equations (5), and (7)-(9)) is a promising powerful tool. Nevertheless this model does not capture the deformations that are imposed on the workpiece, and inevitably affect the accuracy of the manufacturing process. It is therefore desired to extend the fixturing formulation to incorporate models of deformable objects. Thus, an energy based model for optimal fixturing of deformable bodies shall be presented next.

3 The flexible workpiece model for optimal fixturing

3.1 Optimization criteria

The quality and accuracy of manufacturing processes such as drilling or milling depend on the local deformation fields induced in the deformable workpiece by the manufacturing loads. Thus, it is desirable to minimize the manufacturing displacements and angle of rotations in the drilling or milling regions. Such, displacement minimization requires the use of an optimally designed fixture that could provide the necessary kinematic constraints required by the manufacturing process while minimizing the workpiece deformations in the the local domain where the manufacturing process is performed.

In recent years, several objective functions have been proposed aiming at designing optimum fixtures. For example, Lee and Haynes [6] employed an elastic strain energy function minimization to obtain via finite elements optimal three-dimensional fixure configurations. Other optimizing objective functions include a deformation index function, a fixturing force function or a maximum effective stress function aiming at minimizing the damage induced by the manufacturing loads. In this part of the study, an elastic strain energy minimization criterion will be used to assess optimal fixture configurations. For linear elastic systems, the choice of the elastic strain energy function as the optimization objective function is a logical one since at least for the decoupled loading case, it leads to

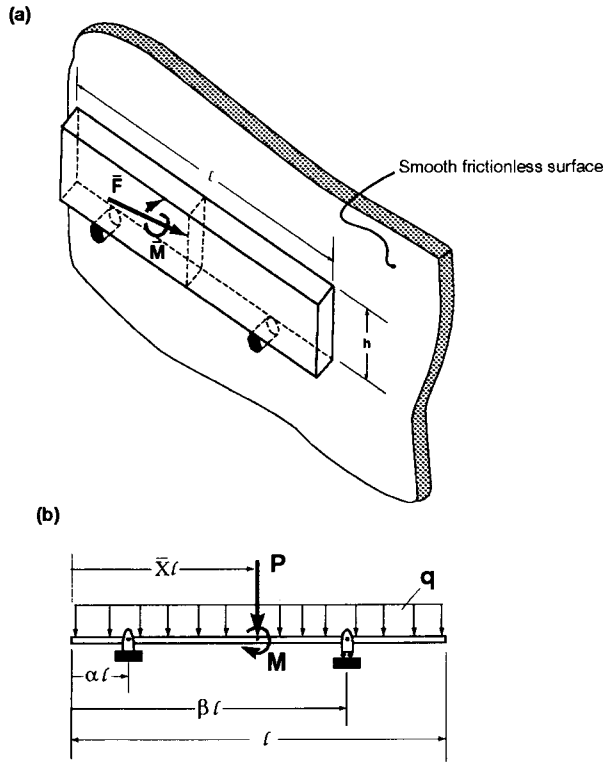

Fig. 6 (a) A slender flexible workpiece subjected to a manufacturing force $\overline{F}$ and bending moment $\overline{M}$. This system is used to develop the mechanical model for optimal fixturing of deformable bodies.
(b) A schematic of the mechanical slender beam model simulating the inclined drilling manufacturing process and fixturing configurations shown in Figure 6a.

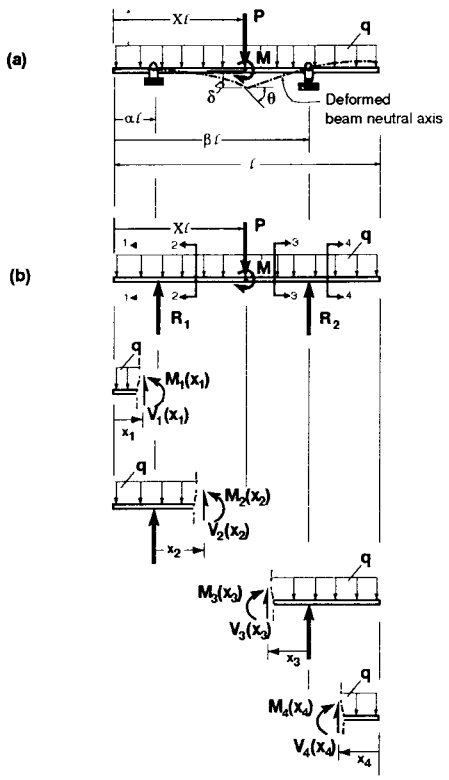

Fig. 7 (a) Deformation components such as the deflection δ and rotation θ of the neutral axis of the slender workpiece shown above, could be used to assess the quality and accuracy of the manufacturing processes performed on flexible workpieces.
(b) Free body diagrams for the entire flexible slender workpiece as well as for parts of the workpiece corresponding to sections 1-1, 2-2, 3-3 and 4-4.

the minimization of the local displacements as shown below.

For linear elastic systems, it can be shown that the elastic strain energy Φ stored in the flexible workpiece is related to the potential work done by the applied loads, Ω, as follows:

$$2\Phi = \Omega \tag{10}$$

where

$$\Phi = \frac{1}{2}\int_V \sigma_{ij}\epsilon_{ij}dV \tag{11}$$

and

$$\Omega = \int_{S_T} \underline{T}\,\underline{u}ds \tag{12}$$

where σ_{ij} and ϵ_{ij} are the components of the stress and strain tensors respectively with the indices i, j varying from 1 to 3, while summation from 1 to 3 is implied over the repeated or dummy indices i and j. Also in the above equations, V denotes the volume occupied by the flexible workpiece whereas S_T denotes the traction boundary over which the tractions $\underline{T}$ induced during manufacturing and other mechanical loads are applied and $\underline{u}$ denotes the displacement vector. The elastic potential energy of the deformable workpiece associated with the manufacturing loads can be obtained in terms of Φ and Ω as follows:

$$\Psi = \Phi - \Omega = -\frac{1}{2}\Omega = -\frac{1}{2}\int_{S_T} \underline{T}\,\underline{u}ds \tag{13}$$

In accordance with equation (12), the potential work done by the applied loads Ω can be obtained in terms

of the applied manufacturing force P and moment M and distributed load q and their work conjucate midplane displacements δ and θ and $u_y(x)$ experienced at their point of applications as shown in Figure 7a. More specifically

$$W = P\delta + M\theta + q\int_0^l u_y(x)dx \tag{14}$$

where

$$\begin{aligned}\delta &= c_{11}P + c_{12}M + c_{13}q \\ \theta &= c_{21}P + c_{22}M + c_{23}q \\ u_y(x) &= c_{31}(x)P + c_{32}(x)M + c_{33}(x)q\end{aligned} \tag{15}$$

In the above deformation expressions, the principle of linear superpoition is used to express the total displacements due to the simultaneous application of the loads, P, M and q via the aid of the compliances c_{ij} i,j=1,2,3 of the flexible system. The system compliances can be obtained either through the Castigliano's energy method approach or by solving for the elastic curve of the beam and then obtaining the displacements and rotations of interest at the manufacturing location. In any case, with the aid of equations, (10) through (15) it becomes clear that when minimizing either the elastic strain energy Φ or the work done by the applied loads Ω or their difference which represents the potential energy of the system Ψ, leads to the minimization of the work conjugate displacements δ^P and θ^M and $u_y(x)$ induced by the decoupled application of the manufacturing loads P and M and the weight of the workpiece q. In the case of coupled loading, i.e., simultaneous application of arbitrary combination of load P, moment M and load intensity q, the energy minimization does not necessarily yield minimum displacements and/or rotation. However, at least when P, M and q are applied independently from one another, and, in order to optimize the fixture for minimum displacements, the elastic strain energy function Φ will be adopted in seeking optimal fixture designs for the manufacturing process performed on a flexible beam as shown in Figure 6a.

3.2 The mechanical model

The model used in this part of the study simulates an inclined drilling manufacturing process on a flexible beam which is laterally fully constrained by a frictionless surface as shown in Figure 6a. It is assumed that the workpiece under consideration has an aspect ratio $h/l \leq 10$, thus rendering a mechanics of materials approach adequate in the energy calculations. For the purpose of this study, all contact surfaces are assumed to be frictionless. Under these conditions, the mechanical model shown in Figure 6b is used to simulate the drilling manufacturing process shown in Figure 6a.

3.3 Elastic strain energy estimates

The elastic strain energy of the flexible beam shown in Figure 6b will be estimated using a mechanics of materials approach. Thus, the shear stress contributions to the elastic strain energy of the systems will be neglected assuming that $h/l \leq 10$. The remaining bending moment contribution can be evaluated as follows:

$$\Phi = \frac{1}{2EI}\int_0^l (M(x))^2 dx \tag{16}$$

where, E is the elastic modulus of the flexible workpiece, $I = bh^3/12$, is the second moment of inertia with respect to the bending axis $z-z$ and $M(x)$ is the bending moment equation as a function of x which measures distances along the axis of the deformable beam. Due to loading discontinuities along the axis x, and due to the discrete kinematic constraints imposed through the fixture support system, the moment equation $M(x)$ is piecewise continues in the interval $0 \leq x \leq l$. When the loads, P, M, q are applied simultanously, the following moment equations are obtained:

$$\begin{aligned}
M_1 &= -\tfrac{1}{2}qx_1^2 && 0 \leq x_1 \leq \alpha l \\
M_2 &= R_1x_2 - \tfrac{1}{2}q(x_2+\alpha l)^2 && 0 \leq x_2 \leq (\bar{X}-\alpha)l \\
M_3 &= R_2x_3 - \tfrac{1}{2}q[x_3+(1-\beta)l]^2 && 0 \leq x_3 \leq (\beta-\bar{X})l \\
M_4 &= -\tfrac{1}{2}qx_4^2 && 0 \leq x_4 \leq (1-\beta)l
\end{aligned} \tag{17}$$

where R_1 and R_2 are the reaction forces which are given by:

$$\begin{aligned}
R_1 &= \tfrac{1}{2(\beta-\alpha)l}\{ql^2(2\beta-1) + 2Pl(\beta-\bar{X}) - 2M\} \\
R_2 &= \tfrac{1}{2(\beta-\alpha)l}\{ql^2(1-2\alpha) + 2Pl(\bar{X}-\alpha) - 2M\}
\end{aligned} \tag{18}$$

With the aid of the above moment equations, the ex-

pression for the elastic energy Φ takes the form:

$$\Phi = \frac{l}{240EI}\frac{1}{\beta-\alpha}\left(\sum_{i=1}^{5} A_i\alpha^{(5-i)} + \sum_{i=1}^{5} B_i\beta^{(5-i)} + \sum_{i=1}^{5} C_i\alpha\beta^{(5-i)} + \sum_{i=1}^{5} D_i\alpha^2\beta^{(5-i)} + E_1\alpha^4\beta\right) \tag{19}$$

where, the index i varies from 1 to 5 and $\sum$ implies summation over the index i of the terms following it. The various constants A_i, B_i and C_i were found to depend on the applied loading and in particular the relative amounts of concentrated force P, moment M and distributed load q and were found to be:

$$\begin{aligned}
A_1 &= 5c_1 + 10c_4 + 10\bar{X}c_5 \\
A_2 &= 0.0 \\
A_3 &= 10c_1 + 40c_2 + 40\bar{X}^2c_3 + 40c_4 + 40\bar{X}c_5 + 80\bar{X}c_6 \\
A_4 &= -6c_1 - 120\bar{X}c_2 - 80\bar{X}^3c_3 - 40\bar{X}^3c_4 - 120\bar{X}c_4 \\
&\quad -60\bar{X}^2c_5 - 10\bar{X}^4c_5 - 240\bar{X}^2c_6 \\
A_5 &= 0.0
\end{aligned} \tag{20}$$

$$\begin{aligned}
B_1 &= -5c_1 - 10c_4 - 10\bar{X}c_5 \\
B_2 &= 20c_1 + 40c_4 + 40\bar{X}c_5 \\
B_3 &= -20c_1 + 40c_2 + 40\bar{X}^2c_3 - 20c_4 - 20\bar{X}c_5 + 80\bar{X}c_6 \\
B_4 &= 6c_1 - 120\bar{X}c_2 - 80\bar{X}^3c_3 - 120\bar{X}^2c_4 + 40\bar{X}^3c_4 \\
&\quad -40\bar{X}^3c_5 + 10\bar{X}^4c_5 - 240\bar{X}^2c_6 \\
B_5 &= 120\bar{X}^2c_2 + 40\bar{X}^4c_3 + 60\bar{X}^2c_4 + 20\bar{X}^3c_5 + 160\bar{X}^3c_6
\end{aligned} \tag{21}$$

$$\begin{aligned}
C_1 &= 10c_1 + 10c_5 \\
C_2 &= -40c_1 - 40c_5 \\
C_3 &= 20c_1 - 80\bar{X}c_3 - 80c_4 + 20c_5 - 80\bar{X}c_5 - 80c_6 \\
C_4 &= 10c_1 + 40c_2 + 160\bar{X}^2c_3 + 240\bar{X}c_4 + 40c_4 \\
&\quad +40\bar{X}c_5 + 120\bar{X}^2c_5 + 320\bar{X}c_6 \\
C_5 &= 0.0
\end{aligned} \tag{22}$$

$$\begin{aligned}
D_1 &= 0.0 \\
D_2 &= 0.0 \\
D_3 &= 40c_1 + 40c_3 + 80c_5 \\
D_4 &= -40c_1 - 80\bar{X}c_3 - 80c_4 - 40c_5 - 80\bar{X}c_5 - 80c_6 \\
D_5 &= 0.0
\end{aligned} \tag{23}$$

and

$$E_1 = -10c_1 - 10c_5 \tag{24}$$

where c_i, $i = 1, 2..6$ are defined as follows:

$$\begin{aligned}
c_1 &= q^2l^4 \\
c_2 &= M^2 \\
c_3 &= P^2l^2 \\
c_4 &= ql^2M \\
c_5 &= ql^3P \\
c_6 &= PlM
\end{aligned} \tag{25}$$

As the next step in this part of the study, the strain energy equation given above will be minimized to identify optimal support locations through the dimensionless parameters α and β, under the constraints imposed by the manufacturing process under consideration. The pertinent constraints in this problem are:

$$\begin{aligned}
&\bar{X} - \alpha \geq 0.05 \\
&\beta - \bar{X} \geq 0.05 \\
&0.0 \leq \alpha \leq \bar{X} \\
&\bar{X} \leq \beta \leq 1.0 \\
&R_1 \neq 0.0 \\
&R_2 \neq 0.0 \\
&|\beta - \alpha| \geq 0.10
\end{aligned} \tag{26}$$

While minimizing the elastic strain energy to obtain optimal fixturing locations, the normal reaction forces corresponding to the optimal energy solutions can be compared to the corresponding reaction forces obtained for all other non-optimal fixture designs. Such

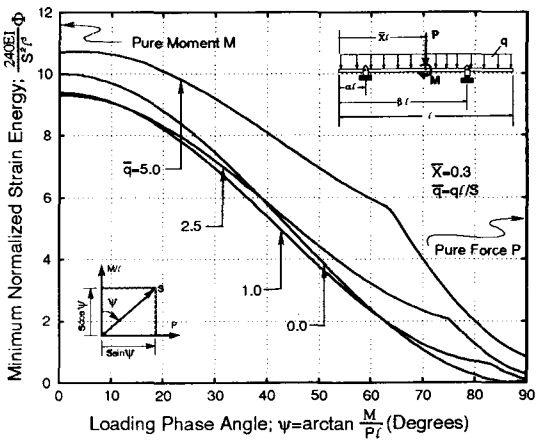

Fig. 8 Trends in the minimum normalized elastic strain energy stored in the deformable workpiece due to the combined application of various amounts of a manufacturing force P and moment M as measured through the loading phase angle ψ.

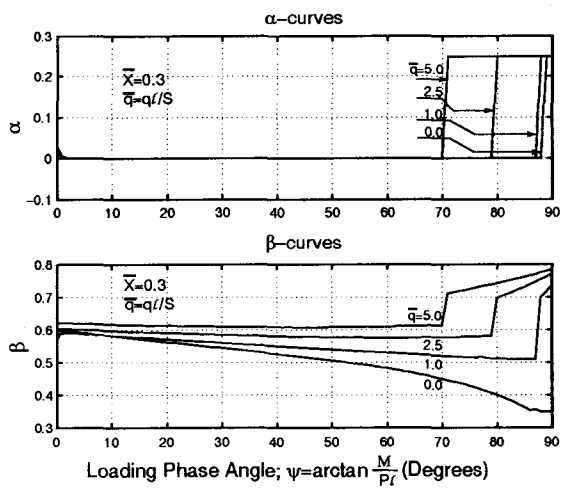

Fig. 9 Optimal locations for the **(a)**-left and **(b)**-right fixturing locations as a function of the loading phase angle ψ. The various curves reflect the effects of superimposing a load intensity q onto the manufacturing loads P and M. The results for $q = 0$ and $\psi = 0°$ correspond to pure bending whereas those for $q = 0$ and $\psi = 90°$ correspond to pure force loading.

a comparison, will test the hypothesis used elsewhere in the literature that minimizing the maximum reaction forces does indeed yield minimum deformations in the elastic workpiece.

4 Results and discussions

As shown schematically in Figure 6b, the load intensity q is used to simulate the weight of the workpiece and possibly other distributed pressure loads externally imposed during the manufacturing process whereas, the loads P and M represent the in-plane components of the inclined manufacturing force $\bar{F}$ and moment $\bar{M}$ shown in Figure 6a. In this work, parameter studies are carried out for the cases wherein the load intensity q is relatively small compared to the manufacturing loads P and M. More specifically, results for normalized workpiece weight $\hat{q} = ql/S = 0.0, 1.0, 2.5$ and 5 are presented. For these cases, the manufacturing loads are assumed to be exerted at a location $\bar{X} = 0.3$ and 0.6. For example, in Figure 8, the minimum normalized elastic strain energy of the flexible workpiece is plotted against the phase angle of loading $\psi = \arctan(\frac{M}{P\ell})$ for $\bar{X} = 0.3$.

As shown schematically in the above figure, the phase angle of loading ψ is used to represent various concentrated force P and bending moment M loading combinations. For example, when $q = 0$, $\psi = 0$ represents a manufacturing process inducing only a pure bending moment loading whereas, $\psi = 90°$, represents a manufacturing process which induces a net in-plane force P while inducing no bending moment. Thus, by introducing the phase angle of loading ψ, the current model, can be used to simulate a wide range of self-similar manufacturing processes. In that respect, the results of this study are general and can be used for the development of improved fixturing for workpieces subjected to the class of manufacturing processes encompassing the entire spectrum of P and M loading combinations.

The results shown in Figure 8, were obtained through a constrained optimization process through which a minimum of the elastic strain energy Φ given by equation (19) was sought by varying the fixturing locations α and β within a kinematically admissible domain under the geometrical and reaction force constraints given by equations (26). The optimum support locations obtained through the above process and which correspond to the optimized energy results re-

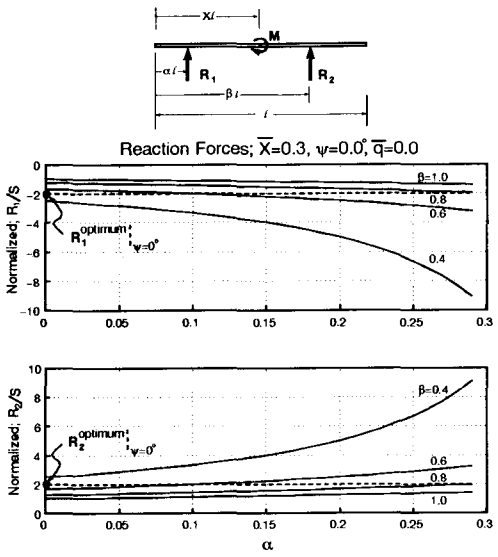

Fig. 10 Non-optimal reaction force predictions as a function of support location measured through the non-dimensional constants α and β. As shown above, these results were obtained, for pure bending loading applied at $\overline{X} = 0.3$. The solid circles represent the respective reaction forces obtained through the energy optimization process.

ported in Figure 8 are shown in Figures 9a and 9b. It is of interest to observe that when the manufacturing process is taking place closer to the left end of the workpiece, i.e., $\bar{X} = 0.3$, the optimum location for the first support is predicted to be $\alpha = 0$. This appears to be the case for all range loading combinations obtained for $\psi < 70°$. In the above phase angle loading regime, and while the optimum α fixturing location is predicted to be at the left end of the workpiece, the β fixturing locations appear to decrease from approximately $\beta = 0.6$ at $\psi = 0°$ to $\beta = 0.45$ at $\psi = 70°$. During the above ψ interval, the optimized elastic strain energy of the deformable workpiece appears to decrease monotonically with ψ at constant S values. Again, in accordance with the moment-force loading sketch shown in Figure 8, S is used to denote an effective loading force magnitude attributed to the manufacturing process. It is also of interest to observe that, when the loading phase angle ψ becomes larger than $\psi = 70°$, the dominance of the concentrated force becomes apparent yielding optimal fixturing solutions at the close proximity of the manufacturing process consistent with the imposed constraints. As discussed earlier in this work, one of the objectives of this second part of the study was to assess the validity of the hypothesis used in the rigid body optimal fixturing modeling, that minimizing the maximum normal reaction force does indeed correspond to minimizing the deformations in the near vicinity of the manufacturing process. In order to test the above hypothesis, the reaction forces R_1 and R_2 given by equations (18) are plotted against all possible α and β values not necessarily corresponding to minimum strain energy. Such results are shown in Figures 10 and 11 which were obtained for a pure bending and pure force loading, i.e., $q = 0$ and $\psi = 0°$ and $\psi = 90°$ respectively. On these plots, the normal reactions forces R_1 and R_2 corresponding to the optimal solutions reported in Figures 9a and 9b are clearly marked using a solid circle. The results shown in Figures 10 and 11, suggest that there exist fixturing solutions other than the energy based optimum solutions that yield normal reaction forces which are smaller than those corresponding to the optimum solution. For example, for pure bending loading, i.e., $\psi = 0°$, and based on the principle of static equilibrium, the reaction forces at the support locations are equal in magnitude and opposite in direction forming a couple opposing the applied moment. Thus, the magnitude of such reaction forces is inversely proportional to the moment arm which in this case would be the support spacing. Consequently, the reaction normal forces reduce as the support spacing increases. Thus, for the system under consideration, under pure bending loading, minimum reaction normal forces obtain when the support or fixturing locations are at the two ends of the flexible beam. The solutions reported in Figures 9a, and 9b suggest that the energy based optimum fixturing locations do not correspond to minimum normal reaction forces. As discussed earlier in this work, for the decoupled loading case, minimizing the elastic energy does correspond to also minimizing the work conjugate deformations. For example, for pure bending loading, the work conjugate displacement would be the angle of rotation at the point of application of the manufacturing loads as shown in figure 7a. Thus, based on the findings of this model, in the pure bending loading case, the hypothesis used by several rigid body fixturing models that minimizing the maximum normal reaction force also minimizes the deformations is proven not to be a valid one. This finding is furthered strengthened through the aid of additional results obtained for the same flexible workpiece subjected to manufacturing loads at a location $\bar{X} = 0.6$. These results which are similar to those reported in Figures 8-11 are reported in Figures 12-15 respectively.

Finally, additional optimal fixturing locations are reported in Figure 16. In this figure, the manufac-

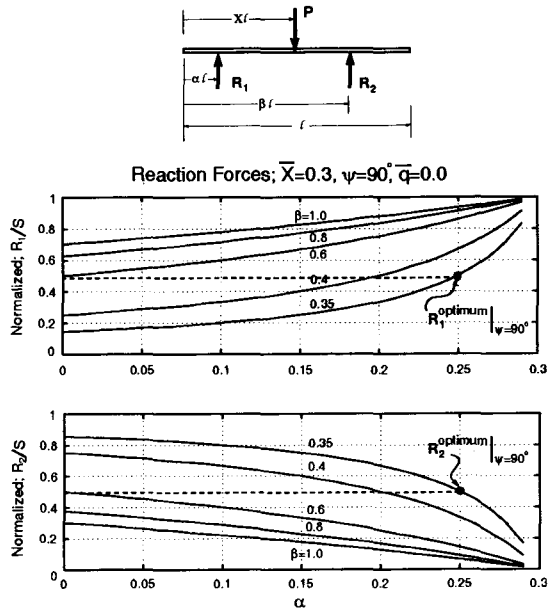

Fig. 11 Non-optimal reaction force predictions as a function of support location measured through the non-dimensional constants α and β. As shown above, these results were obtained, for pure force loading applied at $\overline{X} = 0.3$. The solid circles represent the respective reaction forces obtained through the energy optimization process.

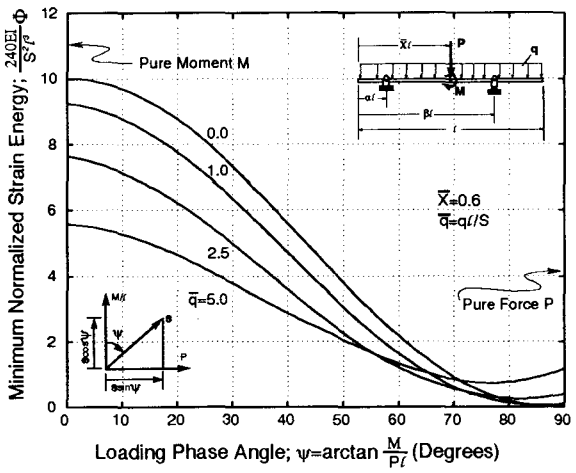

Fig. 12 Trends in the minimum normalized elastic strain energy stored in the deformable workpiece due to the combined application of various amounts of a manufacturing force P and moment M as measured through the loading phase angle ψ. These results are similar to those reported in Figure 8, but were obtained using $\overline{X} = 0.6$.

turing load location as measured through the non-dimensional constant $\bar{X}$ is varied from 0.2 to 0.8. Optimal fixturing locations for α and β are reported in the interval $0 < \psi < 90°$. As expected, manufacturing processes associated with different amounts of force and bending moment require fixturing configurations which may vary substantially for processes inducing bending only to those inducing force loading only.

5 Conclusions

The current manuscript presents an Automatic Fixturing Design (AFD) algorithm that utilizes force closure models of a rigid workpiece. This algorithm turns out to be instrumental in identifying fixtures that possess optimal index values for a given load. The applied load is determined by the manufacturing process that the workpiece is subjected to. Nevertheless, fixture designs have to address accuracy and rigid body models, that do not capture workpiece deformations, cannot predict the workpiece accuracy. This manuscript therefore suggests to incorporate into the AFD algorithm models of deformable bodies. For that purpose, a simple model for optimal fixturing of deformable bodies has also been developed in this manuscript. Optimal fixturing designs have been obtained for a variety of manufacturing processes performed on a flexible and relatively long workpiece. In general, the model suggests that minimizing the strain energy or potential work done by the manufacturing loads does not necessarily minimize the deformations/rotations in the near vicinity of the manufacturing process. In the decoupled loading cases, wherein minimizing the energy also minimizes the work conjugate deformations, the model yielded optimal fixturing configurations which do not necessarily exhibit minimum in the maximum normal reaction force. This suggests that fixture optimization based on rigid body kinematics may not necessarily yield optimal manufacturing processes and thus, under a general state of loading, the elasticity of the workpiece need to be used for optimal fixturing.

6 Acknowledgements

The authors acknowledge the support of the Graduate School of The University of Maryland Baltimore County. Support was also provided by the National

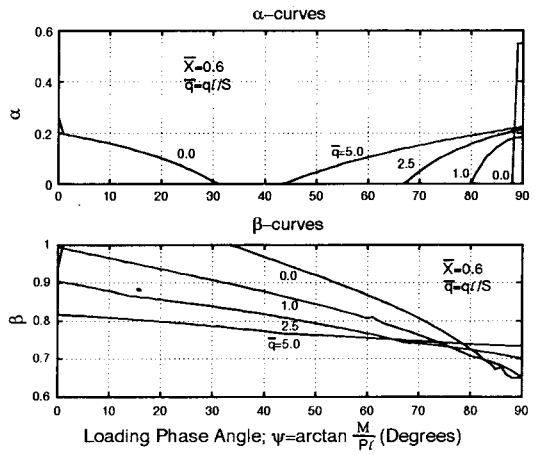

Fig. 13 Optimal locations for the **(a)**-left and **(b)**-right fixturing locations as a function of the loading phase angle ψ. These results are similar to those reported in Figure 9, but were obtained using $\overline{X} = 0.6$.

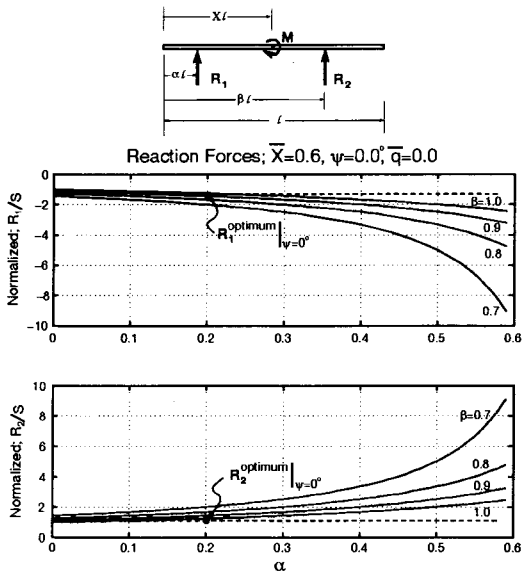

Fig. 14 Non-optimal reaction force predictions as a function of support location measured through the non-dimensional constants α and β. As shown above, these results were obtained, for pure bending loading applied at $\overline{X} = 0.6$. The solid circles represent the respective reaction forces obtained through the energy optimization process.

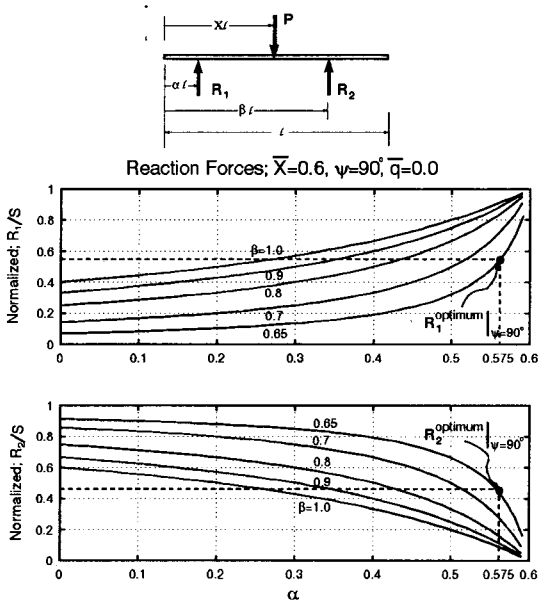

Fig. 15 Non-optimal reaction force predictions as a function of support location measured through the non-dimensional constants α and β. As shown above, these results were obtained, for pure force loading applied at $\overline{X} = 0.6$. The solid circles represent the respective reaction forces obtained through the energy optimization process.

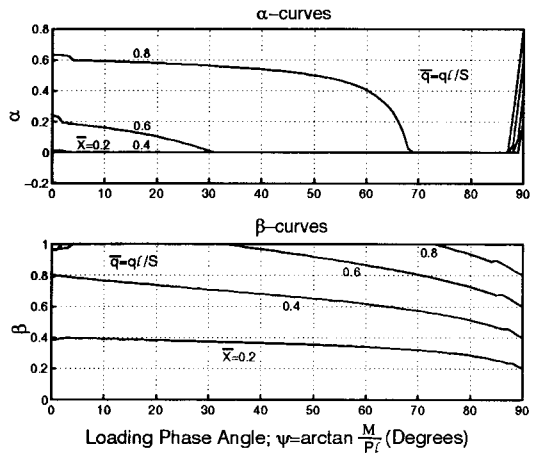

Fig. 16 Optimal locations for the **(a)**-left and **(b)**-right fixturing locations as a function of the loading phase angle ψ. As shown, the various curves correspond to the application of the manufacturing loads at different locations, i.e., $\overline{X} = 0.2,\ 0.4,\ 0.6,$ and 0.8.

Science Foundation through a Presidential Young Investigator's Award, Grant No. MSS-9157090 or CMS-9496209.

References

[1] B. Shirinzadeh, "*Issues in the design of the reconfigurable fixture modules for robotic assembly,*" J. of Manufacturing Systems, 12(1), 1993.

[2] J. Liu and D.R. Strong, "*Sorrey of fixture design automation,*" Vol. 17, No. 4A, 1993.

[3] R.C. Brost, K.Y. Goldberg, "*A complete algorithm for synthesizing modular fixtures for polygonal parts,*" Proc. IEEE Robotics and Automation, San Diego, CA, 1994, pp. 535-542.

[4] V.K. Varma, U. Tasch, "*A New Representation for Robot Grasping Quality Measures,*" Robotica, In Print.

[5] M. Hershkovitz, U. Tasch, M. Teboulle "*Toward Formulation of The Human Grasping-quality Sense* ,"Journal of Robotic Systems, Vol. 12 (4), April 95, pp. 249-256.

[6] J.D. Lee and L.S. Haynes, "*Finite element analysis of flexible fixturing system,*" J. of Engineering for Industry, Vol. 109, pp 134-139, 1987.

[7] R.J. Mencessa and W.R. DeVrice, "*Optimization Methods to Selecting Support Positions in Fixture Design,*" Proc. of the USA-Japan Symposium on Flexible Auto., Vol. 1 Crossing Bridges: Adv. in Flexible Auto & Robotics, July 18-20, 1988.

[8] D.T. Pham and A. Desam Lazoro, "AUTOFIX-An Expert CAD System for Jigs and Fixtures," Int. J. Mach. Tools Manuf. Vol. 30, No. 3, pp. 403-411, 1990.

[9] Z.X. Li, S.S. Sastry, "*Task oriented optimal grasping by multifingered robot hands,*" IEEE Trans. Robotics and Automation, RA-3(4), 1987.

[10] C. Ferrari, J. Canny,"*Planning Optimal Grasps,*" IEEE Conference on Robotics and Automation, Nice France, May 1992, pp. 2290-2295.

[11] Y-C Chou, V. Chandru, M.M. Barash, "*A mathematical approach to automatic configuration of machining fixtures: analysis and synthesis,*" J. of Engineering for Industry, Vol. 111, Nov. 1989.

[12] R. S. Johansson and G. Westling, "Roles of Glabrous skin receptors and sensorimotor memory in automatic control of precision grip when lifting rougher or more slippery objects," *Experimental Brain Research,* 56: 550-564, 1984.

[13] G. Westling and R. S. Johansson, "Factors influencing the force control during precision grip," *Experimental Brain Research,* vol 53, pp. 277-284, 1984.

[14] C. E. Shannon, *Mathematical Theory of Communication,* Bell Sy st. Tech. Journal, 27 (1948), pp. 379-423, 623-656.

[15] J. W. Lee and K. Rim, "Measurements of finger joint angles and maximum finger forces during cylinder grip activity," *Journal of Biomed. Eng.,* Vol. 13, March 1991, pp. 152-162.